Photophysics

International Edition: DOI: 10.1002/anie.201601258
German Edition: DOI: 10.1002/ange.201601258

Intense Ground-State Charge-Transfer Interactions in Low-Bandgap, Panchromatic Phthalocyanine–Tetracyanobuta-1,3-diene Conjugates

Michael Sekita, Beatriz Ballesteros, François Diederich, Dirk M. Guldi, Giovanni Bottari,* and Tomás Torres**

Dedicated to Professor Nazario Martín on the occasion of his 60th birthday

Abstract: *A cycloaddition–retroelectrocyclization reaction between tetracyanoethylene and two zinc phthalocyanines (Zn^{II}Pcs) bearing one or four anilino-substituted alkynes has been used to install a strong, electron-accepting tetracyanobuta-1,3-diene (TCBD) between the electron-rich Zn^{II}Pc and aniline moieties. A combination of photophysical, electrochemical, and spectroelectrochemical investigations with the Zn^{II}Pc-TCBD-aniline conjugates, which present panchromatic absorptions in the visible region extending all the way to the near infrared, show that the formal replacement of the triple bond by TCBD has a dramatic effect on their ground- and excited-state features. In particular, the formation of extremely intense, ground-state charge-transfer interactions between Zn^{II}Pc and the electron-accepting TCBD were observed, something unprecedented not only in Pc chemistry but also in TCBD-based porphyrinoid systems.*

During the last decades, the preparation and study of electron donor–acceptor (D-A) systems exhibiting photoinduced charge separation, a process of paramount importance in natural photosynthesis and solar energy conversion, have gained increasing interest by the scientific community.[1] Among the building blocks used for the construction of such light-powered, electronically active ensembles, phthalocyanines (Pcs) hold a privileged position because of their excellent light-harvesting features, high thermal and photochemical stability, and adjustable redox properties.[2] Up to date, several Pc-based D-A dyads, triads, and more complex arrays have been prepared, in which Pcs, usually acting as light harvester and electron donor, have been connected, covalently or through supramolecular interactions, to electron acceptors of diverse nature and redox character such as carbon nanostructures, perylenediimides, anthraquinones, or porphyrins, to mention just a few.[3] Whereas in the large majority of these Pc-based, D-A conjugates, the formation of charge-separated states is generally observed upon photostimulation, no examples of significant ground-state charge transfer (CT) interactions between the electron donors and the acceptors have been documented to this day. Interestingly, such ground-state CT has been postulated to mediate the charge separation in D-A blends of organic materials in form of a real state, which assists in the separation and recombination of charge-separated states, with a beneficial effect in the photovoltaic performances.[4]

Here, the synthesis and study of two novel D-A conjugates both based on a Zn^{II}Pc covalently connected to one (**1**) or four (**2**) aniline-substituted tetracyanobuta-1,3-diene (TCBD) units are reported. Photophysical and electrochemical investigation carried out on both systems suggest strong electronic communication between Zn^{II}Pc and the electron-accepting TCBD occurring not only in the excited state upon photoexcitation, but also in the ground state. Much to our surprise, low-energy ground-state CT absorptions as intense as the Zn^{II}Pc Q-band (**1**), or even twice as strong (**2**), were observed—a finding, which to the best of our knowledge is unprecedented in Pc chemistry, and, which has not been observed in previously reported TCBD-based porphyrinoid systems.[5]

Conjugates **1** and **2** were prepared in excellent yields, namely 91 % and 95 %, respectively, through a cycloaddition–retroelectrocyclization (CA-RE)[6] reaction of Zn^{II}Pcs **3** and **4** bearing either one or four activated alkynes with electron-deficient tetracyanoethylene (Figure 1).

Interestingly, absorption studies carried out with **1**–**4** showed significant differences between Zn^{II}Pc-TCBD-aniline conjugates **1** and **2** and their Zn^{II}Pc-ethynyl-aniline precursors **3** and **4** (Figure 2). Precursor **3** gives rise to an absorption spectrum in benzonitrile characterized by two main absorptions, namely the B- and the Q-band maximizing at 350 and 696 nm, respectively. In contrast, the absorption spectrum of Zn^{II}Pc-TCBD-aniline **1** presents, in addition to the B- (355 nm) and Q-band (660 nm) transitions, two intense and

[*] Dr. B. Ballesteros, Dr. G. Bottari, Prof. Dr. T. Torres
Departamento de Química Orgánica
Universidad Autónoma de Madrid
Campus de Cantoblanco, 28049 Madrid (Spain)
and
IMDEA-Nanociencia, c/Faraday 9
Campus de Cantoblanco, 28049 Madrid (Spain)
E-mail: giovanni.bottari@uam.es
tomas.torres@uam.es
M. Sekita, Prof. Dr. D. M. Guldi
Department of Chemistry and Pharmacy
Interdisciplinary Center for Molecular Materials (ICMM)
Friedrich-Alexander-Universität Erlangen-Nürnberg
Egerlandstr. 3, 91058 Erlangen (Germany)
E-mail: dirk.guldi@fau.de
Prof. Dr. F. Diederich
Laboratory of Organic Chemistry, ETH Zurich
Vladimir-Prelog-Weg 3, 8093 Zurich (Switzerland)
Supporting information and the ORCID identification number(s) for the author(s) of this article can be found under http://dx.doi.org/10.1002/anie.201601258.

 © 2016 Wiley-VCH Verlag GmbH & Co. KGaA, Weinheim

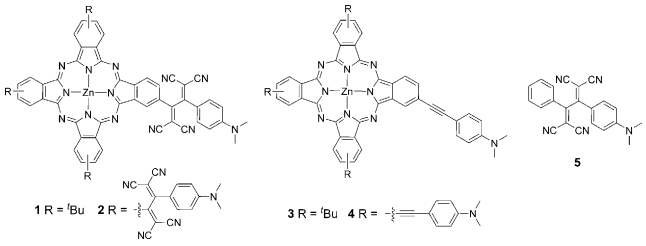


Figure 1. Molecular structures of electron D-A Zn^{II}Pc-TCBD-aniline conjugates **1** and **2**, Zn^{II}Pc-ethynyl-aniline precursors **3** and **4**, and TCBD-aniline derivative **5**.

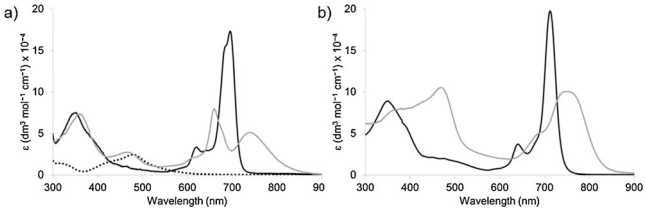


Figure 2. Absorption spectra of D-A Zn^{II}Pc-TCBD-aniline conjugates **1** (a, gray solid line) and **2** (b, gray solid line), Zn^{II}Pc-ethynyl-aniline derivatives **3** (a, black solid line) and **4** (b, black solid line), and TCBD-aniline derivative **5** (a, dotted line) ($c = 1.6 \times 10^{-6}$ M) in benzonitrile.

broad absorptions maximizing at 470 and 752 nm. Similarly, a comparison between the absorption spectra of Zn^{II}Pc-TCBD-aniline **2** and its Zn^{II}Pc-ethynyl-aniline precursor **4** reveals subtle differences. In the former, the B- and the Q-bands, which in **4** are clearly discernable with maxima at 349 and 712 nm, respectively, appear as shoulders at 361 and 685 nm and are accompanied by two intense absorption bands. These dominate the absorption spectrum of **2** with maxima at 470 and 753 nm.[7] These bands are also observed in the absorption spectra of **1** and **2** in toluene and THF (see Figure S13 in the Supporting Information).

To reveal the origin of the intense high- and low-energy absorptions at 470 and 752/753 nm, respectively, observed for Zn^{II}Pc-TCBD-aniline conjugates **1** and **2**, a detailed photophysical and electrochemical investigation of these two D-A conjugates, as well as their precursors **3** and **4**, and TCBD-aniline **5**, deemed necessary.

Valuable insights into the nature of the absorption at 470 nm—as seen for **1** and **2** in benzonitrile—came from the analysis of the absorption spectrum of TCBD-aniline derivative **5**. The latter features a broad absorption maximizing at 478 nm (Figure 2 a). Such transition is attributable in **5** to a CT absorption resulting from ground-state interactions between the electron-donating aniline and the electron-withdrawing TCBD (Figure S30), similarly to what is observed in analogous TCBD-aniline derivatives.[5b,6c] The CT nature of this transition was further confirmed by positive solvatochromism, resulting in a red-shift of the absorption maximum from 462 nm in toluene to 478 nm in benzonitrile, a more polar solvent (Figure S12). In light of the aforementioned, the absorptions of Zn^{II}Pc-TCBD-aniline conjugates **1** and **2** maximizing in benzonitrile at 470 nm are convincingly assigned to the ground-state absorption of the highly-polarized TCBD-aniline fragment. Interestingly, the CT band in (TCBD-aniline)-tetrasubstituted Zn^{II}Pc derivative **2** is nearly four times as intense as in conjugate **1** or derivative **5**, which both contain only one TCBD-aniline fragment. Similar to **5**, conjugates **1** and **2** show a red-shift of the TCBD-aniline-based absorptions upon increasing the solvent polarity from THF to benzonitrile, further supporting the CT nature of these absorptions in these two conjugates (Figure S13).

Somehow different seems the origin of the intense absorptions at 752 and 753 nm observed in benzonitrile for conjugates **1** and **2**, respectively. As a matter of fact, neither the Zn^{II}Pc-ethynyl-aniline precursors **3** and **4** nor the TCBD-aniline derivative **5** disclose any significant absorptions above 720 nm in the same solvent (Figure 2). To exclude that the observed low-energy absorptions in **1** and **2** are the result of a bathochromic shift of the Pc Q-band due to the formation of Zn^{II}Pc *J*-aggregates (Figure S32),[8] on one hand, absorption studies with conjugates **1** and **2** upon adding an excess of pyridine (i.e., 155 equiv) were carried out (Figure S14). Pyridine, which is known to coordinate to the Pc zinc metal center by means of metal-ligand axial coordination, was chosen to rule out possible π-stacking interactions between Zn^{II}Pcs in **1** or **2**. On the other hand, dilution assays in THF of conjugates **1** and **2** were performed (Figures S15 and S16, respectively). The lack of appreciable changes in the position and/or shape of any of the absorption bands either upon dilution or pyridine addition leads us to conclude that intramolecular electronic effects within the Zn^{II}Pc-TCBD-aniline conjugates dominate.

Next, absorption studies of conjugates **1** and **2** in different solvents were carried out indicating a strong influence of the solvent polarity on the low-energy transitions of both compounds with a red-shift of their absorption maxima at 728 nm of about 25 nm when going from THF to benzonitrile (Figure S13 and Table S3). The observed red-shift is taken as a preliminary evidence for a ground-state CT character involving the electron-rich Zn^{II}Pc and the electron-withdrawing TCBD as previously observed in other porphyrinoid-based D-A derivatives.[9] On the other hand, minor changes in the position of the Pc Q-band of **1** and **2** are observed upon changing the solvent polarity, as expected from the "non-polar" nature of this transition (Table S3).

In order to validate this hypothesis, a series of experiments on Zn^{II}Pc-TCBD-aniline conjugates **1** and **2**, as well as their precursors **3** and **4**, and TCBD-aniline **5**, were performed. Firstly, fluorescence assays were carried out and the most relevant data is summarized in Tables S2 and S3. In contrast to Zn^{II}Pc-ethynyl-aniline precursor **3**, which shows a monochromatic, Zn^{II}Pc-centered emission maximizing at 696 nm in toluene, the fluorescence of Zn^{II}Pc-TCBD-aniline conjugate **1** is dual (Figure 3 a). As a matter of fact, the sharp Zn^{II}Pc-centered fluorescence at 695 nm is accompanied by a weaker, broader and featureless emission maximizing at 747 nm. When going to a more polar solvent such as benzonitrile, a further red-shifted, broad, low-energy emission which maximizes at 782 nm is noted for **1** (Figure S17). There is a significant decrease in fluorescence quantum yields when contrasting Zn^{II}Pc-ethynyl-aniline precursor **3** in toluene (0.25) and benzonitrile (0.16), with Zn^{II}Pc-TCBD-aniline

 © 2016 Wiley-VCH Verlag GmbH & Co. KGaA, Weinheim

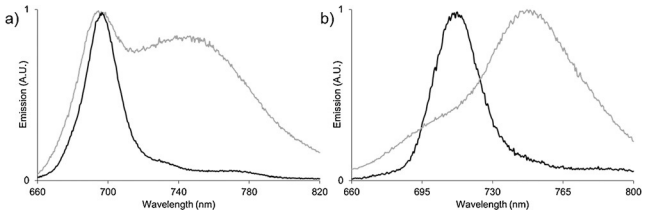


Figure 3. Normalized emission spectra ($\lambda_{exc} = 640$ nm) of a) Zn^{II}Pc-TCBD-aniline conjugate **1** (solid gray line, $c = 6.3 \times 10^{-7}$ M) and Zn^{II}Pc-ethynyl-aniline derivative **3** (solid black line, $c = 2.5 \times 10^{-7}$ M) in toluene and b) Zn^{II}Pc-TCBD-aniline conjugate **2** (solid gray line, $c = 7.84 \times 10^{-7}$ M) and Zn^{II}Pc-ethynyl-aniline derivative **4** (solid black line, $c = 2.5 \times 10^{-7}$ M) in THF.[10]

conjugate **1** in toluene (1×10^{-4}) and benzonitrile (5×10^{-5}; Table S2).

A comparison of the emission features of Zn^{II}Pc-TCBD-aniline conjugate **2** and Zn^{II}Pc-ethynyl-aniline precursor **4** was also carried out in THF and benzonitrile as shown in Figures 3b and S18, respectively. Similarly to **3**, **4** shows a Zn^{II}Pc-centered fluorescence, which maximizes at 711 nm in THF and 719 nm in benzonitrile. In contrast, the Zn^{II}Pc-centered fluorescence of conjugate **2** is quantitatively quenched upon 640 nm excitation. Instead, an extremely broad emission is observable at 748 nm in THF and 782 nm in benzonitrile, which is attributed to CT emission and corresponds to the deactivation of the low-energy transition. Similar to what is observed for **1** and **3**, a pronounced decrease in fluorescence quantum yields of Zn^{II}Pc-TCBD-aniline conjugate **2** with values of $< 5 \times 10^{-5}$ in THF and benzonitrile relative to Zn^{II}Pc-ethynyl-aniline precursor **4** with 0.05 in THF and 0.03 in benzonitrile, was observed (Table S2). Such a significant fluorescence quenching accounts for the strong electronic interaction between Zn^{II}Pc and TCBD.

Next, the redox properties of **1**–**5** were probed by means of cyclic voltammetry (CV) and square wave voltammetry (SWV) in 0.1M *n*-Bu_4NPF_6 CH_2Cl_2 solutions and are summarized in Table S1. All potentials are given vs. the ferrocene/ferrocenium (Fc/Fc^+) couple. TCBD-aniline derivative **5** undergoes an aniline-centered, reversible oxidation at $+0.92$ V and two reversible, TCBD-centered, one-electron reductions at -0.94 and -1.26 V (Figure S5). Zn^{II}Pc-ethynyl-aniline precursor **3** shows three reversible one-electron oxidations at $+0.08$, $+0.30$, and $+0.51$ V and two one-electron reductions at -1.37 and -1.74 V (Figure S8). Four one-electron reductions and two one-electron oxidations are registered for Zn^{II}Pc-TCBD-aniline conjugate **1** (Figure S6). Importantly, the first oxidation of **1** at $+0.37$ V, located on Zn^{II}Pc, is nearly 0.3 V more positive than what is seen in **3**. Such a large difference might be explained considering the strong electron-withdrawing effects exerted by the covalently-linked TCBD on Zn^{II}Pc. A second oxidation at $+0.88$ V, mainly localized on the electron-rich aniline, was also observed for **1**. As for the reduction, it is reasonable to assign the first and second reductions at -0.91 and -1.20 V to TCBD-centered reductions, while the third and fourth reductions at -1.71 and -2.07 V involve Zn^{II}Pc. Electrochemical investigations of **2** and **4** were also carried out. In particular, **4** reveals three oxidations at $+0.02$, $+0.37$, and $+0.57$ V and two Zn^{II}Pc-centered reductions at -1.39 and -1.75 V (Figure S9). Turning to **2**, oxidations at $+0.65$, $+0.81$, and $+1.20$ V and reductions at -0.82 and -1.19 V (TCBD-centered), and -1.80 V (Zn^{II}Pc-centered) were observed (Figure S7). Interestingly, the $+0.65$ V oxidation of **2** present a 0.28 V anodic shift with respect to the first oxidation peak of **1**. This is likely to be a result of increased electron-deficiency of Zn^{II}Pc in **2** the strong electron-withdrawing effect of the four peripheral TCBDs.

As a complement to electrochemical and steady-state fluorescence analyses, and prior to transient absorption studies, spectroelectrochemical experiments on Zn^{II}Pc-TCBD-aniline conjugate **1** and TCBD-aniline derivative **5** were needed to identify the spectral features under reductive and oxidative conditions. Reduction (-0.3 V vs. Ag-wire) of **5** results in the appearance of a minimum at 474 nm due to the decreasing of the characteristic CT band (Figure S10). In parallel, newly developing absorptions maximizing at 393 and 450 nm are observed. They are attributable to the absorption features of the one-electron reduced form of TCBD. Upon reduction (-0.6 V vs. Ag-wire), **1** shows spectroelectrochemical features similar to those detected for **5**, that is, a maximum at 400 nm and a minimum at 466 nm (Figure S11b). In addition, minima at 654 and 741 nm as well as maxima at 613 and 683 nm are observed. On the other hand, upon oxidation ($+0.7$ V vs. Ag-wire), newly developing maxima at 530 and 851 nm and a minimum at 610 nm matches the well-known characteristics of the one-electron oxidized form of Zn^{II}Pc (Figure S11a).[11]

Finally, ultrafast transient absorption experiments with **1**–**5** were carried out in toluene, THF, and benzonitrile. Initially, TCBD-aniline derivative **5** and Zn^{II}Pc-ethynyl-aniline precursor **3** were investigated. Upon 387 or 420 nm excitation of **5** in toluene, differential absorption changes are instantaneously generated with minima in the visible region at 461 nm and near infrared (NIR) region at 1030 nm as well as maxima at 570 and 600 nm (Figures S28 and S29). We attribute these features to a CT excited state. The minimum at 461 nm is a mirror image of the TCBD-aniline ground-state CT absorption. Multiwavelength and global analyses of the transient features reveal a biphasic decay with components of 10.2 and 9.5 ps. As such, both decays are associated with CT and localized transitions, respectively. On the other hand, 660 nm laser excitation of **3** leads to the immediate formation of the Zn^{II}Pc singlet excited-state features with maxima at 455, 476, 493, 599, and 819 nm and minima at 618 and 691 nm (Figure S27a). These features transform to the Zn^{II}Pc triplet excited fingerprints at 487 and 691 nm within 2.4 and 1 ns in toluene and benzonitrile, respectively.

Turning to Zn^{II}Pc-TCBD-aniline derivative **1**, three different excitation wavelengths were used to mainly/selectively pump into 1) the TCBD-aniline CT transition ($\lambda_{exc} =$ 420 nm), 2) the localized Zn^{II}Pc transition ($\lambda_{exc} = 660/694$ nm), and 3) the low-energy band associated with the Zn^{II}Pc-TCBD CT transition ($\lambda_{exc} = 775$ nm).

Firstly, after 420 nm excitation in toluene, newly developing minima at 461, 660, and 740 nm are a good reflection of

 © 2016 Wiley-VCH Verlag GmbH & Co. KGaA, Weinheim

the ground-state absorption (Figures S19a and S20a). These are complemented by transient maxima in the visible at 490 and 548 nm and in the NIR at 1069 nm. Notably, the 490 and 548 nm features in **1** partly relate to that seen upon excitation of the TCBD-aniline CT transition in **5** and the $Zn^{II}Pc$ in **3**. This leaves the latter to originate from $Zn^{II}Pc$-TCBD interactions. As time progresses, that is, 12 ps, a new slight transient maximum is formed at 918 nm. In parallel, the $Zn^{II}Pc$ centered transient at 490 nm diminishes and the visible region is dominated by a broad maximum at 542 nm. Global analysis reveals the presence of an additional 45 ps lived component assigned to a highly polarized $Zn^{II}Pc$-TCBD CT species. A fully charge separated state in the form of the fingerprints of the one-electron oxidized $Zn^{II}Pc$ is, however, not discernable due to a lack of stabilization. As such, excitation into the TCBD-aniline CT transition ultimately acts as an excitation energy sink and, in turn, prevents the population of the charge separated state. Please note that charge separation is, in principle, thermodynamically feasible. Secondly, changing the excitation wavelength to 660 nm (Figures S19b and S20b) leads to the instantaneous formation of the $Zn^{II}Pc$ singlet excited state as evidenced by features in the visible region at 494 and 660 nm. Different from what has been seen for the $Zn^{II}Pc$-ethynyl-aniline precursor **3**, a fast decay within 2 ps sets in for **1** rather than slow intersystem crossing to the triplet excited state. In the process, maxima at 542, 918, and 1069 nm are again observed, which point to the occurrence of $Zn^{II}Pc$-TCBD interactions. Upon decaying, new features, namely 533 and 840 nm maxima and a 610 nm minimum—due to the one-electron oxidized form of $Zn^{II}Pc$—as well as a 425 nm maximum and a 465 nm minimum—because of the one-electron-reduced form of TCBD—are discernible. All of the aforementioned fingerprints grow in with 9 ps in toluene and decay to the ground state with 32 ps. In THF and benzonitrile, the formation and decay are about 2 and 11 ps (Figures S21b and S22a), and about 3 and 25 ps (Figures S23b and S24), respectively. Thirdly, excitation into the $Zn^{II}Pc$-TCBD CT transition at 775 nm (Figure 4) transforms the latter directly into a charge separated state, as also depicted in Figure 5. In this instance, global analyses and

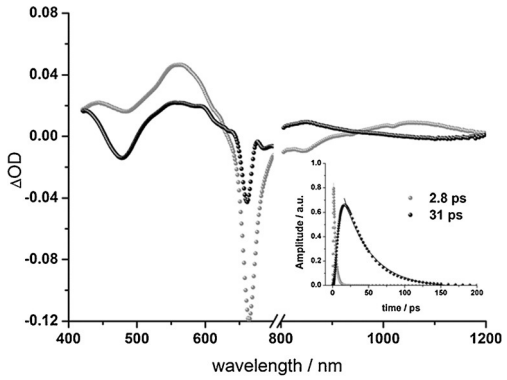


Figure 4. Species-associated spectra and (inset) associated time dependent amplitudes and fits of the femtosecond flash photolysis of $Zn^{II}Pc$-TCBD-aniline **1** (775 nm, 200 nJ) in argon-saturated benzonitrile at room temperature, monitoring the charge separation and charge recombination processes.

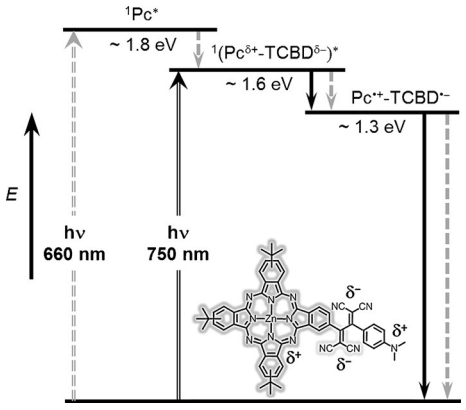


Figure 5. Energy level diagram of $Zn^{II}Pc$-TCBD-aniline conjugate **1** in benzonitrile reflecting energetic pathways of charge separation and charge recombination after excitation of $Zn^{II}Pc$ ($\lambda_{exc}=660$ nm, dashed gray arrows) and $Pc^{\delta+}\text{-}TCBD^{\delta-}$ ground-state CT state ($\lambda_{exc}=750$ nm, solid black arrows). The energy of the polarized $Pc^{\delta+}\text{-}TCBD^{\delta-}$ singlet excited state and $Pc^{\bullet+}\text{-}TCBD^{\bullet-}$ radical ion pair were derived by the CT absorption maximum and by the simple addition of the corresponding redox potentials, that is, oxidation and reduction of **1**, respectively.

multiwavelength analyses reveal like upon 660 nm excitation nearly the same kinetics for charge separation and recombination, respectively (for spectra in toluene and THF see Figures S19c, S20c and S21a, S22b, respectively).

In short, our ultrafast transient absorption experiments are in sound agreement with the emission studies, which indicate that the deactivation of the $Zn^{II}Pc$-TCBD CT excited state into the charge separated state is in competition with a direct deactivation to the ground state. As the solvent polarity is increased, the formation of the charge separated state becomes thermodynamically more favored. Thus, in benzonitrile the 1069 nm feature transforms completely into the 840 nm transient in **1** (Figure 4).

By means of 660 nm excitation, we also probed $Zn^{II}Pc$-TCBD-aniline **2** in THF (Figures S25a and S26a) and benzonitrile (S25b and S26b). Strong electronic coupling between $Zn^{II}Pc$ and TCBD,—as it is discernible in form of CT absorption and emission—is reflected in the NIR region by a broad maximum at 1141 nm, which is 72 nm red-shifted when compared to **1**. A closer global analysis of the differential absorption changes in the visible region recorded after 3 ps in THF and 7 ps in benzonitrile, reveals—like in **1**—fingerprints of the one-electron oxidized form of $Zn^{II}Pc$ and the one-electron reduced form of TCBD. Multiwavelength and global analyses afforded lifetimes for charge recombination to the ground state of 12 ps in THF and 15 ps in benzonitrile (Figure S25c). Please notice again that in benzonitrile, the formation of the charge separated state is favored by virtue of stabilization. On the other hand, next to the features of the charge separation, the 1141 nm feature of **2** in particular in THF points to a direct deactivation of the $Zn^{II}Pc$-TCBD CT excited state into the ground state as an alternative pathway.

At first glance, the simultaneous presence of two intense ground-state CT bands in the absorption spectra of conjugates **1** and **2**, namely $Zn^{II}Pc$-TCBD and TCBD-aniline transitions,

 © 2016 Wiley-VCH Verlag GmbH & Co. KGaA, Weinheim

involving the same TCBD moiety, seems surprising. However, a possible rationale infers from the geometry of **1** and **2**. It is important to consider that TCBD in **1** and **2** is highly nonplanar, with a torsion angle (ϑ) between the four carbon atoms constituting the butadiene backbone. The latter varies between 73 and 127°.[12] For example, the X-ray crystal structure of **5** reveals a ϑ of the TCBD moiety of 83° (Figure S31). As a result of this pronounced twist, no or extremely poor conjugation between the two dicyanovinylene halves of the TCBD fragment is expected to occur in **1** and **2**. This implies that each dicyanovinylene fragment behaves as an independent, electron-withdrawing moiety with respect to the neighboring, electron-rich Zn^{II}Pc and dimethylaniline fragments, resulting in the appearance of two extremely intense ground-state CT bands.

In conclusion, two novel D-A conjugates based on a Zn^{II}Pc as electron donor directly connected to one (**1**) or four (**2**) anilino-substituted TCBD units have been prepared. Both conjugates reveal strong, panchromatic absorptions in the visible region, which extends all the way into the NIR. For these systems, we were able to confirm by means of absorption/emission and electrochemical studies the formation of extremely intense, ground-state CT states, in which Zn^{II}Pcs interact with the electron-accepting TCBD. This is, to the best of our knowledge, unprecedented not only in the context of Pc chemistry but also in TCBD-based porphyrinoids. Transient absorption measurements revealed that the ground-state CT transforms into a charge separated state upon photoexcitation. Overall, 1) the extremely intense ground-state CT, which it has been postulated to contribute to the charge separation in D-A blends of organic materials, 2) the broad and panchromatic absorption in the visible and NIR region, 3) HOMO–LUMO gaps as low as 1.28 eV, and 4) photostimulated electron transfer behavior which also occurs upon excitation into the ground-state CT band render these systems promising materials for applications in the field of molecular photovoltaics.

Acknowledgements

Financial support from the MICINN, Spain (grant number CTQ- 2014-52869-P), the Comunidad de Madrid (grant number S2013/MIT-2841 FOTOCARBON), the EU ("SO2S" FP7-PEOPLE-2012-ITN; grant number 316975) and "Solar Technologies Go Hybrid" network from the Bavarian state is acknowledged. "Universität Bayern e.V." and the Juan de la Cierva Programme of the Spanish MICIMM (grant number JCI-2011-09016) are acknowledged for the support for M.S. and B.B., respectively.

Keywords: charge transfer · donor–acceptor systems · photophysics · phthalocyanines · tetracyanobutadienes

How to cite: *Angew. Chem. Int. Ed.* **2016**, *55*, 5560–5564
Angew. Chem. **2016**, *128*, 5650–5654

[1] a) L. Hammarström, *Acc. Chem. Res.* **2015**, *48*, 840–850; b) A. Arrigo, A. Santoro, F. Puntoriero, P. P. Lainé, S. Campagna, *Coord. Chem. Rev.* **2015**, *304–305*, 109–116; c) S. Fukuzumi, K. Ohkubo, T. Suenobu, *Acc. Chem. Res.* **2014**, *47*, 1455–1464; d) A. Mishra, P. Bäuerle, *Angew. Chem. Int. Ed.* **2012**, *51*, 2020–2067; *Angew. Chem.* **2012**, *124*, 2060–2109; e) D. Gust, T. A. Moore, A. L. Moore, *Acc. Chem. Res.* **2009**, *42*, 1890–1898.

[2] G. de la Torre, C. G. Claessens, T. Torres, *Chem. Commun.* **2007**, 2000–2015.

[3] a) G. Bottari, G. de la Torre, T. Torres, *Acc. Chem. Res.* **2015**, *48*, 900–910; b) G. Bottari, O. Trukhina, M. Ince, T. Torres, *Coord. Chem. Rev.* **2012**, *256*, 2453–2477; c) G. Bottari, G. de la Torre, D. M. Guldi, T. Torres, *Chem. Rev.* **2010**, *110*, 6768–6816; d) F. D'Souza, O. Ito, *Chem. Commun.* **2009**, 4913–4928; e) S. Kirner, M. Sekita, D. M. Guldi, *Adv. Mater.* **2014**, *26*, 1482–1493.

[4] a) A. Y. Sosorev, D. Y. Paraschuk, *Isr. J. Chem.* **2014**, *54*, 650–673; b) C. Deibel, T. Strobel, V. Dyakonov, *Adv. Mater.* **2010**, *22*, 4097–4111; c) K. Akaike, K. Kanai, Y. Ouchi, K. Seki, *Adv. Funct. Mater.* **2010**, *20*, 715–721; d) J. J. Benson-Smith, L. Goris, K. Vandewal, K. Haenen, J. V. Manca, D. Vanderzande, D. D. C. Bradley, J. Nelson, *Adv. Funct. Mater.* **2007**, *17*, 451–457.

[5] a) L. M. Urner, M. Sekita, N. Trapp, W. B. Schweizer, M. Wörle, J.-P. Gisselbrecht, C. Boudon, D. M. Guldi, F. Diederich, *Eur. J. Org. Chem.* **2015**, 91–108; b) F. Tancini, F. Monti, K. Howes, A. Belbakra, A. Listorti, W. B. Schweizer, P. Reutenauer, J.-L. Alonso-Gómez, C. Chiorboli, L. M. Urner, J.-P. Gisselbrecht, C. Boudon, N. Armaroli, F. Diederich, *Chem. Eur. J.* **2014**, *20*, 202–216; c) D. Koszelewski, A. Nowak-Król, D. T. Gryko, *Chem. Asian J.* **2012**, *7*, 1887–1894.

[6] a) T. Michinobu, *Chem. Soc. Rev.* **2011**, *40*, 2306–2316; b) B. Breiten, Y.-L. Wu, P. D. Jarowski, J.-P. Gisselbrecht, C. Boudon, M. Griesser, C. Onitsch, G. Gescheidt, W. B. Schweizer, N. Langer, C. Lennartz, F. Diederich, *Chem. Sci.* **2011**, *2*, 88–93; c) S.-i. Kato, F. Diederich, *Chem. Commun.* **2010**, *46*, 1994–2006.

[7] In the case of Zn^{II}Pc-TCBD-aniline **1** and **2**, a blue-shift of their Q-band was observed with respect to their Zn^{II}Pc-ethynyl-aniline precursors **3** and **4** in all investigated solvents (Table S3). Such hypsochromic shift can be explained considering the reduced π-conjugated surface of the former derivatives with respect to their precursors. In **1** and **2**, the TCBD group connecting the Zn^{II}Pc and the aniline adopts a twisted geometry (see Figure S31), thus hampering the conjugation between these two moieties, which is instead possible in the case of ethynyl-containing derivatives **3** and **4**.

[8] X.-F. Zhang, Q. Xi, J. Zhao, *J. Mater. Chem.* **2010**, *20*, 6726–6733.

[9] a) H. Imahori, N. V. Tkachenko, V. Vehmanen, K. Tamaki, H. Lemmetyinen, Y. Sakata, S. Fukuzumi, *J. Phys. Chem. A* **2001**, *105*, 1750–1756; b) D. M. Guldi, A. Hirsch, M. Scheloske, E. Dietel, A. Troisi, F. Zerbetto, M. Prato, *Chem. Eur. J.* **2003**, *9*, 4968–4979.

[10] Due to the strong fluorescence quenching of Zn^{II}Pc-TCBD-aniline conjugates **1** and **2**, slits of 5 nm were used for the fluorescence experiments with these compounds instead of the 2 nm ones used for compounds **3** and **4**.

[11] J. Bartelmess, B. Ballesteros, G. de la Torre, D. Kiessling, S. Campidelli, M. Prato, T. Torres, D. M. Guldi, *J. Am. Chem. Soc.* **2010**, *132*, 16202–16211.

[12] T. Michinobu, C. Boudon, J.-P. Gisselbrecht, P. Seiler, B. Frank, N. N. P. Moonen, M. Gross, F. Diederich, *Chem. Eur. J.* **2006**, *12*, 1889–1905.

Received: February 3, 2016
Published online: March 24, 2016

 © 2016 Wiley-VCH Verlag GmbH & Co. KGaA, Weinheim